Contrib Mineral Petrol (1998) 132: 139–148

V. Trommsdorff · V. López Sánchez-Vizcaíno
M.T. Gómez-Pugnaire · O. Müntener

High pressure breakdown of antigorite to spinifex-textured olivine and orthopyroxene, SE Spain

Received: 6 February 1998 / Accepted: 24 March 1998

Abstract The prograde, high pressure, transition from antigorite serpentinite to enstatite-olivine rock occurs along a tectonically undisturbed profile at Cerro del Almirez, SE Spain. The reactant assemblage is antigorite + olivine with tremolite rimming precursor diopside. The product assemblage of tremolite + chlorite + enstatite + olivine has a spinifex-like texture with arborescent or radiating olivine elongated parallel to [001] and with radially grown enstatite. Product enstatite is very poor in Al_2O_3. Due to numerous oriented submicroscopic inclusions of chromian magnetite, product olivine has a brownish pleochroism and a bulk chromium content similar to precursor antigorite. Titanian clinohumite with a fluorine content of 0.45–0.50 wt% persisted beyond the breakdown of antigorite. The partitioning of iron and magnesium amongst the silicate phases is almost identical to that at lower pressures. Average K_d values Mn/Mg and Ni/Mg are 0.17 and 0.70 for antigorite-olivine pairs and 1.83 and 0.22 for orthopyroxene-olivine pairs, respectively. These data are useful in discriminating generations of olivine grown on each other. From the field data a phase diagram topology for a portion of the system CaO-MgO-SiO_2-H_2O is derived. This topology forms the basis for extrapolations into inaccessible *P-T* regions.

V. Trommsdorff (✉) · O. Müntener
Institut für Mineralogie und Petrographie, ETH Zentrum, CH-8092 Zürich, Switzerland

V. López Sánchez-Vizcaíno
Depto. Geologia, Escuala Universitaria Politécnica, Universidad de Jaen, E-23700 Linares, Spain

M.T. Gómez-Pugnaire
Depto. Mineralogia y Petrologia, Facultad de Ciencias, Universitad de Granada, E-18002 Granada, Spain

Editorial responsibility: J. Hoefs

Introduction

Subduction of serpentinized lithospheric mantle is considered an important process, because its dehydration provides a source of H_2O that may trigger partial melting and affect rheological and seismic properties of mantle rocks. The knowledge of phase relations in subducting serpentinite is important for monitoring these processes. Therefore, in recent years, a great number of experimental studies have been carried out in order to determine high pressure phase relations of hydrous ultramafic systems (Yamamoto and Akimoto 1977; Pawley and Wood 1995, 1996; Wunder and Schreyer 1997; Bose and Ganguly 1995; Ulmer and Trommsdorff 1995). Attempts to model these systems thermodynamically for pressures and temperatures corresponding to various subduction zone environments (Evans and Guggenheim 1988; Pawley and Wood 1995) have been only partly successful and are faced with increasing difficulties, particularly at high pressures, because of the lack of relevant thermodynamic data. In contrast to experimental work and thermodynamic modelling the field evidence for high pressure metamorphism of serpentinite has received relatively little attention. For example, the major sources of H_2O in subducting hydrous mantle, the breakdown reactions of antigorite and talc have been studied repeatedly in experiments and theory but only a part of them have been recovered in the field. The relative stability fields of talc and antigorite parageneses, which are crucial in evaluating the phase relations of subducting serpentinites, are only incompletely known for parts of the lithosphere. Trommsdorff and Evans (1972, 1974) demonstrated that at moderate pressures of up to ~10 kbar antigorite breaks down to forsterite + talc at temperatures below 600 °C. Depending on pressure this product assemblage is then consumed by various dehydration steps until the ultimate product, enstatite + olivine, is formed. According to experimental studies (Ulmer and Trommsdorff 1995; Wunder and Schreyer 1997) and internally

consistent thermodynamic data (Berman et al. 1986; Berman 1988) the intermediate dehydration products are absent at high pressures and antigorite breaks down directly to enstatite + olivine. Although antigorite is known to exist to conditions of eclogite facies (Bearth 1967; Evans 1977; Scambelluri et al. 1995), the direct breakdown of antigorite to enstatite + olivine remains to be demonstrated in the field (Evans and Guggenheim 1988, p. 267). This breakdown reaction, however, is considered to be a major source of H_2O for calc-alkaline magmatism (Ulmer and Trommsdorff 1995). It is the purpose of this study to present a case where this reaction can be demonstrated in the field and to derive from the relations of phases coexisting in the field a phase diagram topology relevant for ultramafic rocks.

Geological setting

The studied ultramafic rocks belong to the Nevado-Filábride Complex, the lowermost tectonic complex of the Internal Zones of the Cordilleras Béticas (Fig. 1). They are tectonically emplaced in the upper part (Mulhacén Unit) of this complex. The ultramafics are on the top of a sequence thinned by extensional tectonics. This sequence consists of white micaschists, quartzites and occasional marble lenses, that overlie graphite-bearing micaschists and quartzites which are considered to be of Paleozoic age. Late brittle contacts separate the ultramafic rocks from the other rock types. During the Alpine Orogeny the Mulhacén Unit underwent a Paleogene compressional event, in which *HP* conditions (about 2.0 GPa and 500–600 °C) were reached (Gómez-Pugnaire and Fernández-Soler 1987). Exhumation during the Oligocene was essentially decompressive, with a metamorphic peak at about 0.6 GPa and 600–650 °C (Nijhuis 1964; Gómez-Pugnaire and Fernández-Soler 1987; Bakker et al. 1989). The exhumation path passed through greenschist facies conditions during the Burdigalian. Subsequently, an important extensional event took place which obliterated most of the previous structures. This event is responsible for the present position of the ultramafic rocks (García Dueñas et al. 1992; González Lodeiro et al. 1996).

The ultramafic rocks from the Almirez area that display a well-developed spinifex-like texture were originally interpreted as the product of near surface crystallization of a crystal-melt mush of harzburgitic composition that was quickly quenched and then partly transformed into antigorite serpentinite (Burgos et al. 1980; Morten and Puga 1984; Puga 1990). A secondary, metamorphic origin for the spinifex-like texture was later proposed by Bodinier et al. (1993) and by Puga et al. (1995, 1997) on basis of the chemical features and by Müntener et al. (1997) on the basis of phase relations.

The ultramafic rocks

The ultramafic rocks of Cerro del Almirez (Jansen 1936) form three major bodies that are parts of a thrust sheet covering an area of three km^2 (Fig. 1). The ultramafic thrust sheet is about 400 m thick and is built up of two rock types. One of them occurs in the upper 200 m of the Cerro del Almirez mountain and is formed of schistose antigorite serpentinite. The second, tectonically lower rock type is more massive and forms various enstatite-forsterite rocks in which the arborescent, radiating, spinifex-like textures dominate (Fig. 2). The two minor ultramafic bodies west of the Cerro del Almirez (Fig. 1) also belong to this rock type. The contact between the two rock types is sharp but irregular and shows no evidence of a tectonic discontinuity.

A localized faint banding is recognised in all ultramafic rocks. The banding results from alternating cm to dm thick layers varying in clinopyroxene content. In places clinopyroxenite up to 1 m thickness occurs. Rodingite boudins, which in places cross the layering, occur over the entire ultramafic body. Titanian clinohumite occurs as knobs or deformed veins together with diopside and olivine in the serpentinites and locally as specks in the enstatite-olivine rocks.

The assemblage of rocks in the serpentinite part of Cerro del Almirez is identical to that of many antigorite serpentinites in the Penninic zone of the Alps (Bearth 1967).

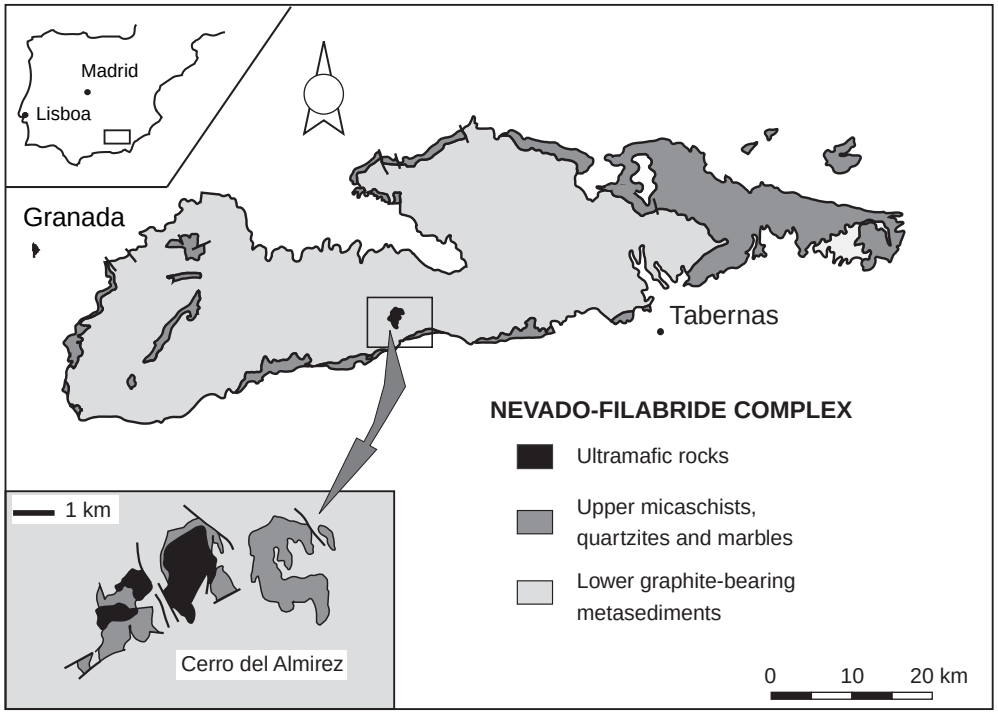

Fig. 1 Outline geological map of the Nevado Filábride Complex with Cerro del Almirez details

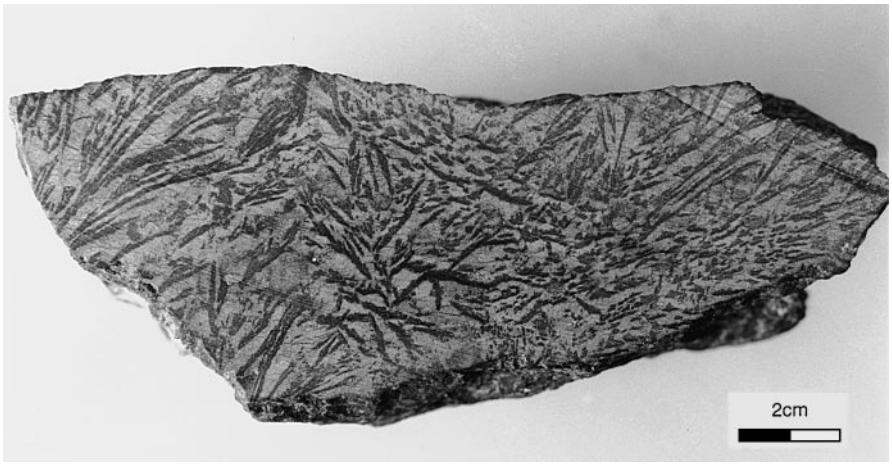

Fig. 2 Spinifex-like, arborescent olivine (*dark*) in an enstatite + chlorite ± tremolite matrix. Field of view 13 × 7 cm

Petrography

Serpentinites

These are made up of a schistose assemblage of antigorite, olivine and diopside, with minor chlorite and discontinuous strings of magnetite. Accessory minerals are pentlandite, pyrrhotite, ilmenite, and titanian clinohumite. Premetamorphic cores of dusty clinopyroxene and of olivine are not uncommon in larger individual crystals. Tremolite associated with olivine is widespread, and frequently rims diopside (compare Plate I A, B in Trommsdorff and Evans 1974), indicating that the reaction

$$\text{diopside} + \text{antigorite} = \text{tremolite} + \text{olivine} + H_2O \quad (1)$$

has taken place. Breakdown of OH-titanian clinohumite has been observed locally:

$$\text{titanian clinohumite} = \text{olivine} + \text{geikielite/ilmenite} + H_2O \quad (2)$$

which according to Trommsdorff and Evans (1980) takes place at moderate pressures under the same conditions as reaction (1).

In pyroxenitic layers in the antigorite serpentinites, i.e. antigorite-chlorite-tremolite-diopside rocks, zirconium-rich domains have been found in which zirconolite, zircon and baddeleyite coexist with olivine plus ilmenite. They will be the subject of a separate paper.

Enstatite-olivine rocks

These rocks in the lower part of the sequence (Fig. 3) occur in two varieties: the predominant variety is characterized by a spinifex-like texture, whereas the second variety has a granular texture. The mineralogical composition of both rock types is essentially the same. The assemblage consists of olivine, enstatite, chlorite, tremolite and chromian magnetite. Accessory minerals, in some instances also in major quantities, are pyrite, pyrrhotite, pentlandite, ilmenite and titanian clinohumite. In contrast to the antigorite serpentinites chlorite is quite abundant.

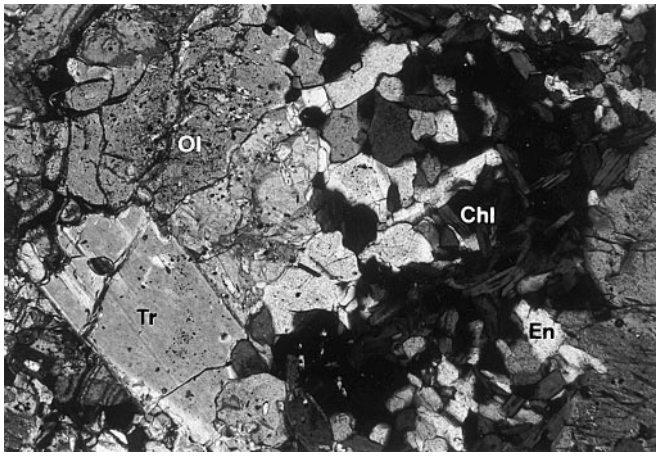

Fig. 3 The product assemblage enstatite-olivine-chlorite-tremolite. Olivine is cut *perpendicular to elongation*. Mineral abbreviations after Kretz (1983). Field of view 1.35 × 0.93 mm

Olivine in the enstatite-olivine rocks occurs in three generations (Fig. 4) that overgrow each other. The first, serpentinite stage, generation forms irregular shaped clear cores within elongate cm-size porphyroblastic spinifex-like olivine which constitutes a second generation. This second, enstatite-olivine stage, generation has a brownish pleochroism and is dusty with small inclusions of chlorite and smaller chromian magnetite. The brownish colour results from numerous oriented submicroscopic inclusions of chromian magnetite, in some cases concentrated in lamellae parallel to (001) and (100). Second generation olivine in places overgrows folded strings of magnetite which are typical for the precursor serpentinite (similar to Plate IC, Trommsdorff and Evans 1974). The third generation of olivine is texturally late, in part granoblastic and minor in size. In the spinifex-like rocks brownish olivines dominate in size and quantity and are up to 10 cm in length. The elongation direction is [001]. Enstatite occurs in two gener-

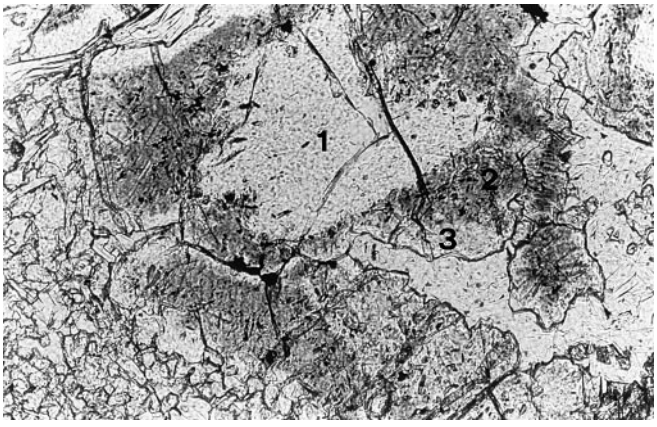

Fig. 4 Three generations of olivine. The *clear core* is inherited from antigorite serpentinite, generation (*1*); the *dusty zone* is spinifex-like olivine with numerous inclusions of chlorite and chromian magnetite (*2*) and the *clear rim* is recrystallized olivine belonging to the granoblastic generation (*3*). Field of view 1.20 × 0.83 mm

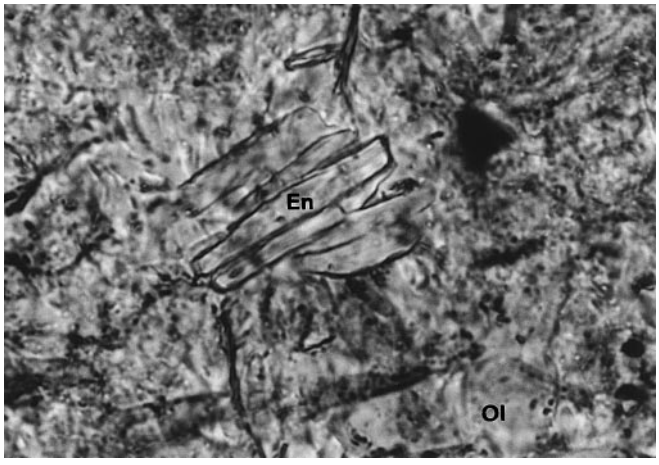

Fig. 6 "Baby enstatite" in centre of elongate olivine. Field of view 0.14 × 0.10 mm

ations. The first of these is radiating (Fig. 5), with a grain size of typically 1 cm, and frequently contains tiny inclusions of chlorite. The second generation of enstatite is represented by small granoblastic grains. Simultaneous crystallization of both spinifex-like olivine and radiating enstatite is suggested by frequent parallel intergrowth of these minerals and by the occurrence of idioblastic microinclusions of enstatite in the cores of brownish olivine (Fig. 6). Tremolite occurs as individual crystals and as radial aggregates and in more pyroxenitic layers comprises up to 10% of the rock. In addition to its occurrence as inclusions, chlorite forms fine grained interstitial aggregates associated with chromian magnetite and enstatite.

Titanian clinohumite is found only locally as granoblasts several mm in size, typically associated with ilmenite, chlorite and chromian magnetite. Breakdown of titanian clinohumite to wormy intergrowths of olivine plus ilmenite is observed in some samples.

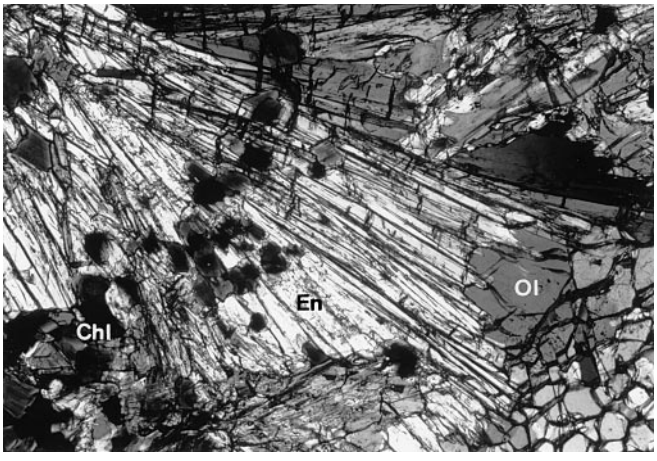

Fig. 5 Radiating enstatite in spinifex-like rock. Field of view 2.7 × 1.9 mm

Among secondary minerals talc is typically replacing enstatite and can reach considerable quantities although it is largely absent from the unaltered rocks. A later local product is secondary chrysotile close to the borders of the ultramafic bodies. No antigorite replacing the enstatite-olivine assemblage has been observed (cf. Puga 1990), but some antigorite bordering chlorite in retrograde talc-rich rocks has been found.

The granoblastic variety of enstatite-olivine rock is considered to be derived from the spinifex-like variety through deformation. It is concentrated in shear bands within the latter rocks in which many relicts of brownish olivine are observed. Radial enstatite on the other hand survived the deformation and remains surrounded by granoblastic olivine and enstatite (Fig. 5).

Mineral compositions

The Table summarizes typical microprobe analyses of the metamorphic minerals from Cerro del Almirez. Although the overall variations in mineral composition of the various rock types are small there are some notable differences.

Olivine

In terms of iron-magnesium ratios *olivine* varies from Fo 89 to 92, whereas the other minerals show maximum variations in X_{Mg} of 0.01. The order of preference of Fe for the different minerals is similar to the values given by Trommsdorff and Evans (1972, 1974). There is a tendency that all the Mg-silicates are somewhat less Fe-poor relative to olivine than in Trommsdorff and Evans. For Fo 90 the composition of coexisting minerals, expressed as X_{Mg}, are (Fig. 7): enstatite 0.90; antigorite 0.93; chlorite 0.94; diopside 0.96 and tremolite 0.965. Retrograde talc has a constant X_{Mg} of 0.98.

Table 1. Representative analyses of minerals from antigorite serpentinites (Al–95–20), and olivine-enstatite rocks (Al 95–4d, Al 95-R2). [X_{Mg} is Mg atoms/(Mg + Fe + Mn + Ni) atoms]

Sample	Olivine enstatite rock (Al95–4d)						Olivine-enstatite rock (Al95-R2)				Tremolite-bearing serpentinite (Al95–20)					Average. relative error (2σ) in %
Weight %	Ol (core)	Ol (brown)	Opx	Tr	Chl	Mag	TiCl	Ol	Opx	Chl	Ol	Atg	Tr	Di	Mag	
SiO_2	40.7	40.1	58.8	58.6	33.1	< 0.03	36.4	40.5	57.4	33.7	41.6	41.2	57.8	54.8	< 0.03	0.6 (at 40% level)
TiO_2	< 0.02	< 0.02	< 0.02	< 0.02	< 0.02	0.49	4.87	< 0.02	0.05	< 0.02	< 0.02	< 0.02	< 0.02	< 0.02	0.13	8.2 (at 0.05% level)
Cr_2O_3	< 0.03	< 0.03	0.17	< 0.03	2.35	6.90	0.11	< 0.03	0.15	1.06	< 0.03	0.49	< 0.03	< 0.03	2.10	4.4 (at 0.4% level)
Al_2O_3	< 0.03	< 0.03	0.25	0.19	13.7	0.21	< 0.03	< 0.03	0.21	13.0	< 0.03	3.89	0.78	< 0.03	0.03	2.0 (at 4% level)
Fe_2O_3[a]						59.8									67.3	
FeO	9.57	8.93	6.18	1.34	3.49	30.7	8.99	10.23	7.18	3.87	6.58	3.65	1.18	0.79	29.0	3.0 (at 7% level)
NiO	0.35	0.44	0.07	0.09	0.29	0.38	0.31	0.42	0.06	0.22	0.24	0.18	0.05	< 0.05	0.21	9.6 (at 0.2% level)
MnO	0.23	0.15	0.19	0.06	< 0.03	0.15	0.10	0.07	0.13	0.03	0.36	0.05	0.06	0.09	0.28	3.8 (at 0.35% level)
MgO	49.0	50.1	35.6	23.9	34.3	1.02	47.6	48.7	34.7	35.1	51.5	38.1	23.9	18.1	1.14	1.4 (at 20% level)
CaO	< 0.02	< 0.02	0.11	13.1	< 0.02	< 0.02	< 0.02	< 0.02	0.05	< 0.02	< 0.02	< 0.02	13.3	25.9	< 0.02	1.2 (at 10% level)
Na_2O	< 0.03	< 0.03	< 0.03	0.31	< 0.03	< 0.03	< 0.03	< 0.03	< 0.03	< 0.03	< 0.03	< 0.03	0.33	< 0.03	< 0.03	10.6 (at 0.2% level)
K_2O				0.08	< 0.02					< 0.02						12.0 (at 0.1% level)
H_2O calc				2.20	12.64		1.44			12.64		12.01	2.19			
F							0.45									1.6 (at 0.45% level)
Σ	99.9	99.7	101.4	99.9	99.9	100.2[b]	100.1	99.9	99.9	99.6	100.3	99.6	99.6	99.7	100.2	
Ions calculated on the basis of 3 cations (olivine, spinel), 6 oxygens (orthopyroxene), 23 oxygens and Fe3/Fetotal = 0 (amphibole), 36 oxygens (chlorite), 147 oxygens (antigorite) and 13 cations (titanian clinohumite)																
Si	1.000	0.980	1.997	7.986	6.290	0.000	3.982	0.995	1.987	6.400	1.004	31.896	7.905	1.992	0.000	
Ti	0.000	0.000	0.001	0.002	0.003	0.014	0.400	0.000	0.001	0.000	0.000	0.006	0.001	0.000	0.004	
Cr	0.001	0.000	0.005	0.000	0.353	0.207	0.010	0.000	0.004	0.159	0.000	0.298	0.003	0.001	0.063	
Al	0.000	0.000	0.010	0.031	3.054	0.010	0.000	0.000	0.009	2.912	0.000	3.551	0.125	0.000	0.001	
Fe3						1.705									1.928	
Fe2	0.196	0.182	0.176	0.152	0.554	0.974	0.822	0.210	0.208	0.613	0.133	2.365	0.135	0.024	0.923	
Ni	0.007	0.009	0.002	0.010	0.044	0.012	0.027	0.008	0.002	0.034	0.005	0.112	0.005	0.001	0.007	
Mn	0.005	0.003	0.006	0.007	0.000	0.005	0.009	0.002	0.004	0.004	0.007	0.031	0.007	0.003	0.009	
Mg	1.789	1.823	1.800	4.853	9.701	0.058	7.748	1.784	1.790	9.937	1.850	43.903	4.861	0.983	0.064	
Ca	0.000	0.000	0.004	1.907	0.001	0.000	0.000	0.000	0.002	0.004	0.000	0.000	1.943	1.007	0.001	
Na	0.002	0.000	0.000	0.082	0.000	0.000	0.000	0.000	0.000	0.000	0.000	0.026	0.087	0.000	0.000	
K				0.015	0.000					0.000						
OH				2.000	16.000		1.047			16.000		62.000	2.000			
F							0.156									
X_{Mg}	0.896	0.904	0.907	0.966	0.942	0.055	0.900	0.890	0.893	0.939	0.927	0.946	0.971	0.972	0.064	

[a] Calculated assuming stoichiometry
[b] Sum includes 0.56 wt% V_2O_3

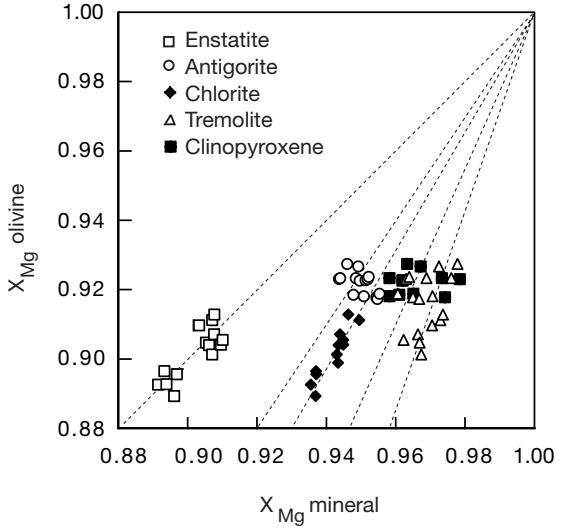

Fig. 7 Partitioning of Mg between olivine and other silicates [X_{Mg} Mg atoms/(Mg + Fe + Mn + Ni) atoms]. *Dotted lines* are eye ball fits

The generations of metamorphic olivine are distinguishable on the basis of their forsterite contents. Olivine in the serpentinites has Fo 0.92 ± 0.007. In enstatite-olivine rocks the brown elongate generation spans a range from Fo 89 to 91.5 with the clear cores clustering around Fo 89.5. The neoblast generation is distinctly more magnesian with Fo 91–91.5.

Antigorite

This is quite similar to typical antigorite from Alpine ultramafic rocks (Trommsdorff and Evans 1972) with the exception of trivalent cations which are distinctly higher and range up to over 4 wt% Al_2O_3 and to 0.58 wt% Cr_2O_3. For example, antigorite Al 95–20 (Table) contains 28 mol% of chlorite component with a composition of those reported for Al 95–4d. The capacity of antigorite to accommodate trivalent cations appears to be maximized at high temperature in the stability field of the tremolite-olivine- antigorite assemblage and near its breakdown. In view of the quite high pressures of over 1.5 GPa at Cerro del Almirez the antigorite breakdown is also at distinctly higher temperatures (≥650 °C) than in the Bergell aureole (Trommsdorff and Connolly, 1996, 530 °C at 0.35 GPa.)

Orthopyroxene

This mineral occurs only in the lower section of the Almirez ultramafics and is En_{90} Fs_{10}. The radial enstatite reaches a maximum of 0.6 wt% Al_2O_3 in its core and the later, granoblastic, generation has < 0.1 wt% Al_2O_3, comparable to enstatite-chlorite-forsterite schists of the Central Alps. The zonation of the enstatite in terms of trivalent cations with higher contents in the core and lower ones in the rims is considered to be retrograde in origin.

Clinopyroxene and tremolite

Both these are close to the pure endmember compositions with low contents of trivalent cations and with a tendency to accommodate some alkalis (diopside up to 0.6 wt% and tremolite up to 0.10 wt% Na_2O; K_2O in tremolite < 0.10 wt%). In tremolite coexisting with olivine, enstatite and titanian clinohumite traces of fluorine have been detected (< 0.05 wt%).

Chlorite

Chlorite in the spinifex-like rocks is comparable to that in enstatite-chlorite-olivine schists (Trommsdorff and Evans 1974) with high magnesium contents, Cr_2O_3 up to 3 wt% and Al_2O_3 from 12 to 15 wt%.

Titanian-clinohumite

This mineral in the serpentinites is close to the pure (OH)-end-member. In the spinifex-like rocks it typically contains about 0.5 wt% of fluorine and 4.8–5 wt% TiO_2 which translates into $X_{Ti} = 0.4$, where X_{Ti} = Ti p.f.u. of 13 cations; and $X_F = 0.1$, where $X_F = F/(F+OH)$ and $X_{Ti} + X_F = 0.5$. The measured titanian clinohumites are quite homogeneous in their F/Ti ratio and contain systematically about 0.1 wt% Cr_2O_3.

Chromian magnetite

Chromian magnetite in the spinifex-like rocks is titanium poor (Fenoll Hach-Ali et al. 1991), low in Al_2O_3 (< 2 wt%) and MgO (< 1.5 wt%). The Cr_2O_3 reaches 12 wt% equivalent to 16 wt% of chromite component. The composition compares well with chromian magnetites of tremolite-chlorite-enstatite-olivine rocks from the Central Alps (Evans and Frost 1975, p. 966, analysis n. 4).

Compared to these chromian magnetites the submicroscopic inclusions in olivine seem to contain more Cr_2O_3 and similarly low titanium (semiquantitative energy dispersive transmission electron microscope analysis).

The chemical discrimination of different mineral generations on the basis of minor elements is most obvious in the case of the olivine. This is shown in Fig. 8 where the cation proportions of Ni and Mn are plotted against each other. Olivine from serpentinites is lowest in Ni and highest in Mn; the opposite is true for the large dusty spinifex-like olivine. The clear cores of spinifex-like olivine plot nicely in an intermediate position between these two extremes and the recrystallized genera-

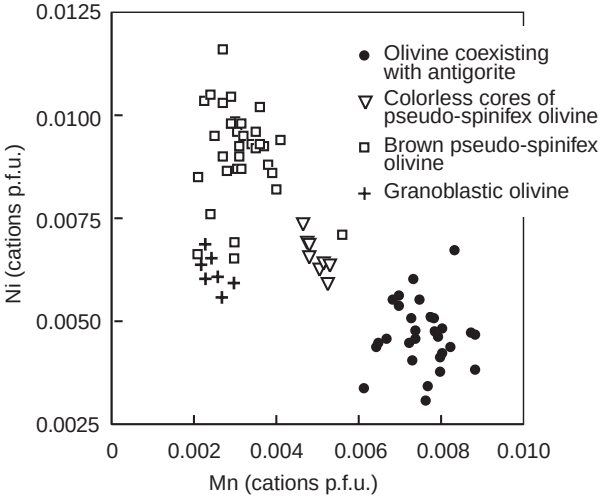

Fig. 8 Ni versus Mn for olivine generations of the serpentinite and the spinifex-like rocks

tion of granoblastic clear olivine has, compared to the spinifex-like one, lower Ni contents. Olivine that coexists with secondary talc spans the range of all generations of the spinifex-like rocks. In sample Al 95-4D a threefold zoned single olivine grain shows clearly the variations (Fig. 9) as discussed above for the whole range of data. The average distribution coefficients (K_D) for Mn/Mg and Ni/Mg for antigorite/olivine pairs are typically 0.17 and 0.70 respectively, and for orthopyroxene/olivine pairs in the spinifex-like rocks 1.83 and 0.22 respectively.

The breakdown of antigorite

The breakdown of antigorite at Cerro del Almirez can be described by an overall mass-balance of the type

$$\text{antigorite} = \text{enstatite} + \text{olivine} + \text{chlorite} + H_2O \quad (3)$$

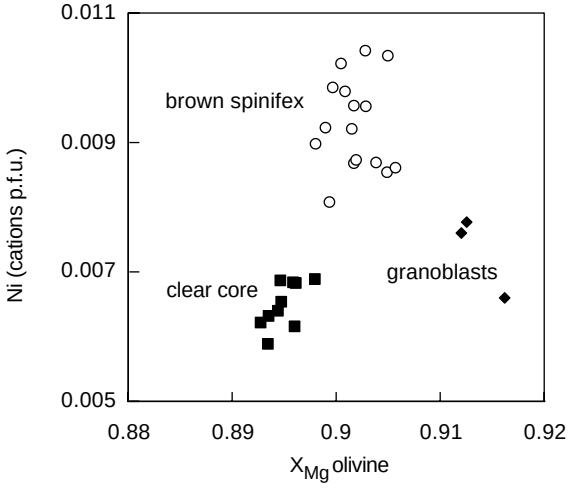

Fig. 9 X_{Mg} versus Ni (cations per formula unit) for three olivine generations in one grain of spinifex-like olivine [X_{Mg} Mg atoms / (Mg + Fe + Mn + Ni) atoms]. (Sample Al-95–4d)

which occurs entirely within the stability field of tremolite plus olivine. Because the product assemblage can also be attained through two intermediate steps (Trommsdorff and Evans 1974, p. 64)

$$\text{antigorite} = \text{talc} + \text{olivine} + \text{chlorite} + H_2O \quad (4)$$

and

$$\text{talc} + \text{olivine} = \text{enstatite} + H_2O \quad (5)$$

arguments and evidence for reaction (3) are here listed in detail. They are as follows:

1. The boundary between serpentinite and pseudospinifex chlorite-enstatite-olivine rocks is sharp, but irregular, with no intermediate tectonic discontinuity. The two rock types grade into each other over a distance of no more than a few tens of metres. No intermediate talc zone is observed.
2. Pseudospinifex olivine in places overgrows folded strings of magnetite which are typical for the precursor serpentinite.
3. Parallel growth of arborescent olivine and radiating enstatite indicates simultaneous crystallization. If enstatite grew from talc, olivine would be consumed (reaction 5) and not produced.
4. Chlorite occurs as inclusions in pseudospinifex olivine and enstatite and is far more abundant than in the serpentinites. The clear relic olivine cores are free of chlorite inclusions.
5. The elongation of pseudospinifex olivine is parallel to [001] and not parallel to [010] as observed in the talc-olivine spinifex-like rocks (Evans and Trommsdorff 1974).
6. The submicroscopic inclusions in pseudospinifex olivine are chromian magnetites poor in titanium. The quantity of chromium in olivine plus microinclusions is approximately equivalent to that of the precursor antigorite. Antigorite does not accommodate any titanium.
7. Nickel content in spinifex-textured olivine is higher than in olivine of the serpentinites which is opposite to what is observed in olivine + talc rocks growing from serpentinite. The reason for this is that talc incorporates relatively high quantities of Ni but enstatite does not.
8. Manganese is concentrated in olivine of the serpentinites, but in enstatite of the spinifex-like rocks. Thus Mn is low in spinifex-like olivine which is not the case in olivine of talc + olivine rocks.

Evaluation of the stable phase diagram topology for CaO-MgO-SiO_2-H_2O

Because of unresolved differences in the experimental data on antigorite breakdown [Evans et al. 1976; Ulmer and Trommsdorff 1995 (natural antigorite); Wunder and Schreyer 1997 (synthetic, pure antigorite)] and uncertainties in the various thermodynamic data bases due to an undefined structural state of antigorite and lack of an appropriate model for the high pressure and high temperature volumetric properties of tremolite (Comodi

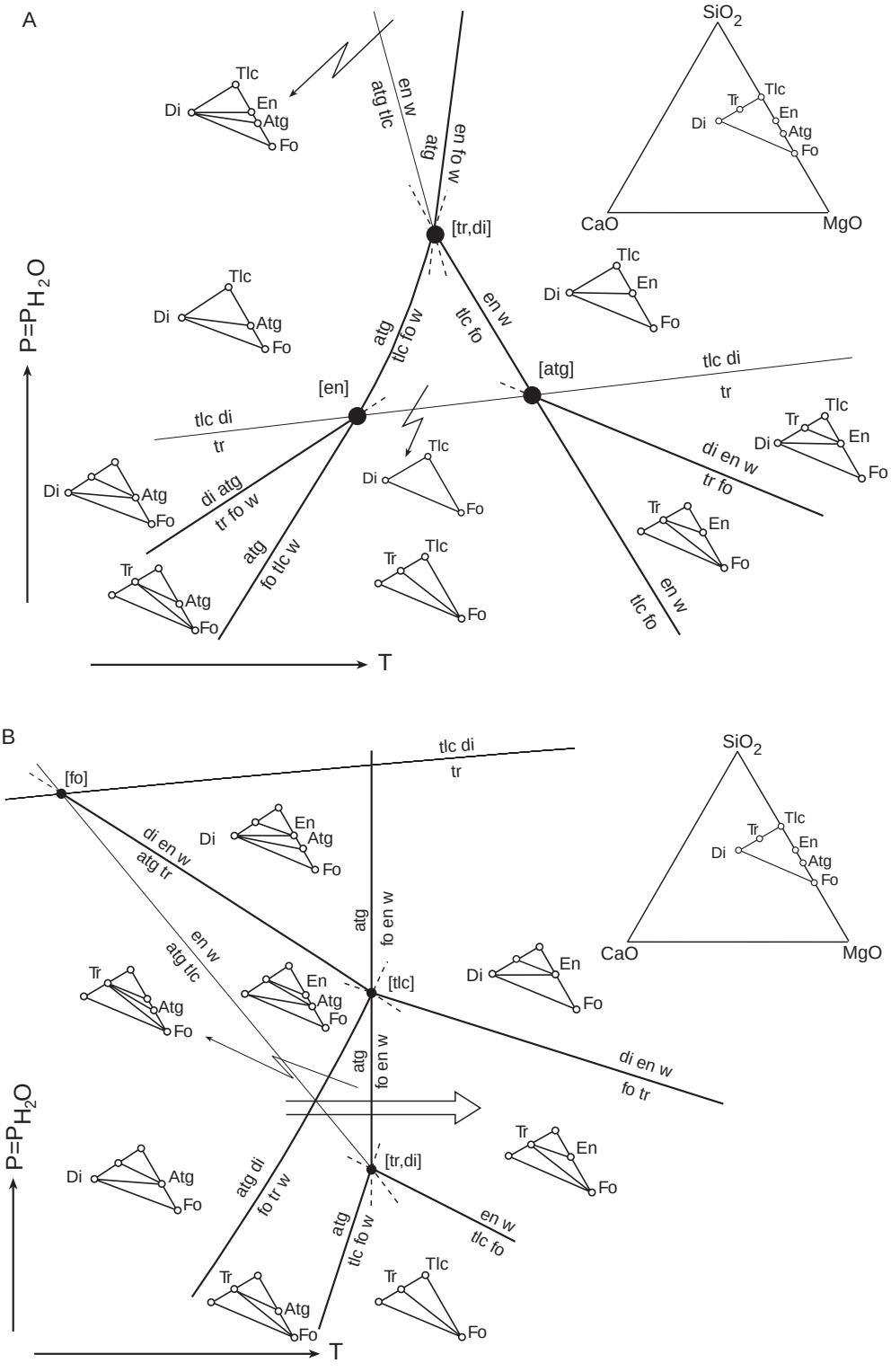

Fig. 10A, B Phase diagram topologies for a portion of the system CaO-MgO-SiO_2-H_2O, defined by the *apices* diopside, talc and forsterite and projected from H_2O. *Thin lines* are for bulk compositions that do not encounter the join forsterite-antigorite. A Topology that was not encountered at Cerro del Almirez. B Topology fitting the phase relations of Cerro del Almirez with the prograde sequence encountered shown by an arrow

et al. 1991; Berman 1988; Holland and Powell 1990) and talc (Bose and Ganguly 1995, cf. Pawley et al. 1995) it is impossible to derive a relevant phase diagram topology for the system merely on the basis of experimental and thermodynamic data. However, the evidence discussed in this paper permits derivation of the stable phase relations among natural antigorite, forsterite, enstatite, talc, tremolite and diopside. These phase relations are constrained by the prograde sequence of isograd reactions encountered at low to moderate pressures (Evans et al. 1976), and those encountered at high pressure at Cerro del Almirez. Taking the sequence derived by

Evans et al. (1976) and stability of the *equilibrium* involved in reaction (3)

$$\text{antigorite} = 10\ \text{enstatite} + 14\ \text{forsterite} + 31\ H_2O \quad (6)$$

as given, two topologies are possible for the system as shown in Fig. 10 A and B. In both topologies the invariant point [tr, di] is stable (abbreviations after Kretz 1983) at which antigorite, olivine, talc and enstatite coexist with an H_2O-fluid. In topology A additional invariant points [en] and [atg] are stable and [fo] and [tlc] are metastable. The inverse is true for topology B. However, only topology B satisfies the phase relations observed at Cerro del Almirez, because tremolite coexists with the assemblage given by reaction (3). The alternative topology requires, instead of tremolite, stability of diopside + talc which has not been observed.

The prograde sequence of Cerro del Almirez must occur between the invariant points [tr, di] and [tlc] as indicated by an arrow on Fig. 10B. These points fall between temperatures of 640 and 720 °C and 1.5–2.2 GPa (Point [tr, di]) and 1.8–2.2 GPa (Point [tlc]), taking into consideration the various data bases and experimental determinations.

Summary and conclusions

The situation encountered at Cerro del Almirez allowed us to demonstrate for the first time in the field that the breakdown of antigorite to orthopyroxene plus olivine has taken place. The reactants developed distinctive textures with arborescent olivine elongated parallel to [001] and radial enstatite. Jackstraw (criss-cross) textured olivine elongated parallel to [001] and in association with enstatite has been described from the Norwegian Caledonides by Bakke and Korneliussen (1986) where the authors assumed a serpentinite protolith but did not discuss the reaction path to the final orthopyroxene plus olivine rock. Elongation of olivine parallel to [001] is also typical for spinifex textures developed in komatiites (Dickey 1972). Olivine growing according to the breakdown of antigorite to olivine plus talc in some cases is elongated parallel to [010] and tabular parallel to (100) (Evans and Trommsdorff 1974). Snoke and Calk (1978) suggested that the habit of olivine may be an indicator of the physical conditions of crystallization. For all the occurrences of elongate olivine textures the presence of abundant fluid seems critical, independent of whether olivine growth was metamorphic (Evans and Trommsdorff 1974; Snoke and Calk 1978) or magmatic (Grove et al. 1996; Parman et al. 1997). For the breakdown of antigorite at Cerro del Almirez the presence of an abundant, H_2O dominated, fluid phase is assumed in view of the 12 wt% H_2O liberated by this reaction.

The topology derived here from field relationships for high pressure antigorite rocks is strictly valid only for the fluid and the mineral compositions encountered at Cerro del Almirez. In view of the fact that these minerals are close to the Mg-endmember compositions the pressure/temperature shift in dehydration equilibria due to impurities is trivial with respect to an ideal, pure system. On the other hand, considerable pressure shifts have been calculated for the *intersections* of such equilibria which determine the topology of the phase diagram (Evans and Guggenheim 1988). It may, however, be noted that the topology relevant for Cerro del Almirez is also obtained for the pure system with the data base of Berman (1988, modified 1996).

Many arguments and evidence have been given in this paper for the breakdown of antigorite to enstatite plus olivine. However, unless the breakdown is mappable it may not be easy to find proof for this reaction in other field areas. In most of the metamorphic enstatite-forsterite rocks of the Central Alps enstatite can be found which contains aligned inclusions of tiny olivine (Trommsdorff and Evans 1974, Plate I, E) which indicates growth of enstatite from precursor olivine-talc or olivine-Mg-amphibole rocks. Additional arguments for the alternative breakdown reaction are to be found if bulk compositions are considered that are more siliceous than normal ultramafic rocks (see Fig. 10B); where antigorite and enstatite can coexist.

The persistence of titanian clinohumite in the stability field of enstatite plus olivine at Cerro del Almirez is consistent with its occurrence in high pressure peridotites as well as with recent experimental investigations (Weiss 1997). Although beyond the scope of this paper it may be stated on the basis of the observed phase relations for the Cerro del Almirez rocks that maximum metamorphic pressures were in excess of 1.5 GPa and temperatures in excess of 640 °C. This is consistent with field evidence cited in the geological introduction.

Evidence from nature, as presented here, may be considered as a starting point for the modelling of phase relations in hydrous ultramafic rocks for pressure temperature regimes that are otherwise inaccessible.

Acknowledgements This paper has been reviewed by Bernard Evans, Jamie Connolly, Giovanni Piccardo and Peter Ulmer. We thank all these colleagues and the Schweizerischer Nationalfonds (project no. 2000-050454.97/1) as well as Grupo Junta Andalucia RNM-0145 and CICYT Project PB 96-1266 and University of Jaén (travel grant) for their support.

References

Bakke S, Korneliussen A (1986) Jack-straw-textured olivines in some Norwegian metaperidotites. Nor Geol Tidsskr 66: 271–276

Bakker HE, Jong K de, Helmers H, Biermann C (1989) The geodynamic evolution of the Internal Zone of the Betic Cordilleras (south-east Spain): a model based on structural analysis and geothermobarometry. J Metamorphic Geol 7: 359–381

Bearth P (1967) Die Ophiolithe der Zone von Zermatt-Saas-Fee. Beitr Geol Karte Schweiz, N F 132

Berman RG (1988) Internally consistent thermodynamic data for minerals in the system Na_2O-K_2O-CaO-MgO-FeO-Fe_2O_3-SiO_2-TiO_2-H_2O-CO_2. J Petrol 29: 445–522

Berman RG, Engi M, Greenwood HJ, Brown TH (1986) Derivation of internally-consistent thermodynamic data by the tech-

nique of linear programming, a review with applications to the system MgO-SiO_2-H_2O. J Petrol 27: 1331–1364
Berman RG, Arenovich L Ya (1996) Optimized standard state and solution properties of minerals I. Contrib Mineral Petrol 126: 1–24
Bodinier JL, Puga E, Díaz de Federico A, Leblanc M, Morten L (1993) Secondary harzburgites with spinifex-like textures in the Betic Ophiolitic Association (Southeastern Spain)(abstract). Terra Abstr 5: 3
Bose K, Ganguly J (1995) Experimental and theoretical studies of the stabilities of talc, antigorite and phase A at high pressures with applications to subduction processes. Earth Planet Sci Lett 136: 109–121
Burgos J, Díaz de Federico A, Morten L, Puga E (1980) The ultramafic rocks from the Cerro del Almirez, Sierra Nevada Complex, Betic Cordilleras, Spain: preliminary report. Cuad Geol 11: 157–165
Comodi P, Mellini M, Ungaretti L, Zanazzi PF (1991) Compressibility and high pressure structure refinement of tremolite, pargasite and glaucophane. Eur J Mineral 3: 485–500
Dickey JS (1972) A primary peridotite magma – revisited: olivine quench crystals in a peridotite lava. In: Shagam R, et al; (eds) Studies in Earth and space sciences. Geol Soc Am Mem 132: 289–297
Evans BW (1977) Metamorphism of alpine peridotite and serpentinite. Annu Rev Earth Planet Sci 5: 397–447
Evans BW, Frost BR (1975) Chrome-spinel in progressive metamorphism – a preliminary analysis. Geochim Cosmochim Acta 39: 959–972
Evans BW, Guggenheim S (1988) Talc, pyrophyllite, and related minerals. In: Bailey SW (ed) Hydrous phyllosilicates. (Reviews in mineralogy, 19) Mineral Soc Am, Washington, DC, pp 225–294
Evans BW, Trommsdorff V (1974) On elongate olivine of metamorphic origin. Geology 2: 131–132
Evans BW, Johannes W, Oterdoom H, Trommsdorff V (1976) Stability of chrysotile and antigorite in the serpentinite multisystem. Schweiz Mineral Petrogr Mitt 56: 79–93
Fenoll Hach-Ali P, Gervilla F, Puga E, Díaz de Federico A (1991) Mg-ilmenite and other Fe-Ti oxides in high-pressure metamorphic rocks from the Betic Ophiolitic Association, Southern Spain (abstract). Terra Abstr 3: 112
García Dueñas V, Balanyá JC, Martínez Martínez JM (1992) Miocene extensional detachments in the outcropping basement of the northern Alborán Basin (Betics) and their tectonic implications. Geo-Mar Lett 12: 88–95
Gómez-Pugnaire MT, Fernández Soler JM (1987) High-pressure metamorphism in metabasites from the Betic Cordilleras (SE Spain) and its evolution during the Alpine orogeny. Contrib Mineral Petrol 95: 231–244
González Lodeiro F, Aldaya F, Galindo-Zaldívar J, Jabaloy A (1996) Superposition of extensional detachments during the Neogene in the Internal Zones of the Betic Cordilleras. Geol Rundsch 85: 350–362
Grove TL, Gaetani GA, Parman SW, Dann JC, Wit MJ de (1996) Origin of olivine spinifex textures in 3.49 Ga komatiite magmas from the Barberton mountainland, South Africa. EOS Trans Am Geophys Union 77: 281
Holland TJB, Powell R (1990) An enlarged and updated internally consistent dataset with uncertainties and correlations: the system K_2O-Na_2O-CaO-MgO-MnO-FeO-Fe_2O_3-Al_2O_3-TiO_2-SiO_2-C-H_2-O_2. J Metamorphic Geol 8: 89–124
Jansen H (1936) The geology of Sierra de Baza and adjacent areas of the Sierra Nevada and Sierra de los Filabres. PhD thesis, Amsterdam Univ, Netherlands
Kretz R (1983) Symbols for rock-forming minerals. Am Mineral 68: 277–279
Morten L, Puga E (1984) Blades of olivines and orthopyroxenes in ultramafic rocks from the Cerro del Almirez, Sierra Nevada Complex, Spain: relics of quench-textured harzburgites? Neues Jahrb Mineral Mohnats 1984: 211–218
Müntener O, Trommsdorff V, López Sánchez-Vizcaíno V, Gómez Pugnaire MT (1997) High pressure breakdown of antigorite serpentinite to olivine-enstatite spinifex-like textured rocks, Sierra Nevada, SE Spain (abstract). Terra Abstr 9: 21
Nijhuis HJ (1964) Plurifacial alpine metamorphism in the southeastern Sierra de los Filabres, south of Lubrín. PhD thesis, Amsterdam Univ, Netherlands
Parman SW, Dann JC, Grove TL, Wit MJ de (1997) Emplacement conditions of komatiite magmas from the 3.49 Ga Komati formation, Barberton greenstone belt, South Africa. Earth Planet Sci Lett 150: 303–323
Pawley AR, Wood BJ (1995) The high-pressure stability of talc and 10 Å phase: potential storage for H_2O in subduction zones. Am Mineral 80: 998–1003
Pawley AR, Wood BJ (1996) The low-pressure stability of phase A, $Mg_7Si_2O_8(OH)_6$. Contrib Mineral Petrol 124: 90–97
Pawley AR, Redfern SAT, Wood BJ (1995) Thermal expansivities and compressibilities of hydrous phases in the system MgO-SiO_2-H_2O: talc, phase A and 10Å phase. Contrib Mineral Petrol 122: 301–307
Puga E (1990) The Betic ophiolitic association (southeastern Spain). Ofioliti 15: 97–117
Puga E, Díaz de Federico A, Leblanc M, Morten L, Jelloul M, Bodinier JL (1995) Oceanic serpentinization and rodingitization processes in the ultramafic sequence of the Betic ophiolite association (Mulhacen complex, SE Spain) (abstract).In: 2nd workshop on orogenic lherzolites and mantle processes, Granada 1995, pp 51
Puga E, Díaz de Federico A, Bodinier JL, Morten L, Nieto JM (1997) High-pressure metamorphism in the Betic ophiolitic association (Betic Cordilleras, SE Spain) (abstract). Terra Abstr 9: 26–27
Scambelluri M, Müntener O, Hermann J, Piccardo GB, Trommsdorff V (1995) Subduction of water into the mantle: history of an Alpine peridotite. Geology 23: 459–462
Snoke AW, Calk LC (1978) Jackstraw-textured talc-olivine rocks, Preston Peak area, Klamath Mountains, California. Geol Soc Am Bull 89, 223–230
Trommsdorff V, Connolly JAD (1996) The ultramafic contact aureole about the Bregaglia (Bergell) tonalite: isograds and a thermal model. Schweiz Mineral Petrogr Mitt 76: 537–547
Trommsdorff V, Evans BW (1972) Progressive metamorphism of antigorite schist in the Bergell Tonalite aureole (Italy). Am J Sci 272: 423–437
Trommsdorff V, Evans BW (1974) Alpine metamorphism of peridotitic rocks. Schweiz Mineral Petrogr Mitt 54: 334–352
Trommsdorff V, Evans BW (1980) Titanian hydroxyl-clinohumite: formation and breakdown in antigorite rocks (Malenco, Italy). Contrib Mineral Petrol 72: 229–242
Ulmer P, Trommsdorff V (1995) Serpentine stability to mantle depths and subduction-related magmatism. Science 269: 858–861
Weiss M (1997) Clinohumites: a field and experimental study. PhD diss, ETH Zürich, no. 12202
Wunder B, Schreyer W (1997) Antigorite: high-pressure stability in the system MgO-SiO_2-H_2O (MSH). Lithos 41: 213–227
Yamamoto K, Akimoto SI (1977) The system MgO-SiO_2-H_2O at high pressures and temperatures – stability field for hydroxylchondrodite, hydroxyl-clinohumite and 10Å phase. Am J Sci 277: 288–312